Al-Khwarizmi Engineering Journal

Al-Khwarizmi Engineering Journal
ISSN (printed): 1818 – 1171, ISSN (online): 2312 – 0789
Vol. 22, No. 3, September, (2026), pp. 89–99

Depth-Based Feature Recognition of Blind Pockets and Islands from STEP AP242 CAD Models for Milling Applications

Amirulihsan Mohamad[1], Zammeri Abd Rahman[2*], Saiful Bahri Mohamed Mohamad[3], Muhammad Haziq Omar[4], Razwan Rohimi[5], Muhammad Abdulrahim Rabbani Md Sharizam[6], Tengku Mohd Sharir Tengku Sulaiman[7], Mohamad Minhat[8] and Wawan Trisnadi Putra[9]

[1,2,3,4,5,6,7]*Design Optimization and Manufacturing Research Group, Faculty of Innovative Design and Technology, Universiti Sultan Zainal Abidin, Kampus Gong Badak, 21300 Kuala Nerus, Terengganu, Malaysia*

[8]*Faculty of Manufacturing Engineering, Universiti Teknikal Malaysia Melaka, Hang Tuah Jaya, 76100 Durian Tunggal, Melaka, Malaysia*

[9]*Faculty of Engineering, Universitas Muhammadiyah Ponorogo, Ponorogo 63471, Indonesia*

*Corresponding Author's E-mail: zammeri@unisza.edu.my

(Received 16 July 2025; Revised 7 February 2026; Accepted 15 June 2026; Published 1 September 2026)
https://doi.org/10.22153/kej.2026.06.002

Abstract

The identification of blind pocket and island features in modern computer-aided design (CAD) and in the manufacturing of 3D CAD models is crucial. It ensures the accuracy and efficiency in the computer numerical control (CNC) machining process. These features often pose challenges for automated detection. This study proposes an automated method for detecting blind pockets and islands in Standard for the Exchange of Product Model Data (STEP) AP242 files using a depth-based approach. The methodology involves analysing geometric information from the STEP file, arranging regions by depth (Z-values) and recognising between blind pocket and island features. The approach uses a series of geometric algorithms to detect edges, vertices and surfaces, followed by the identification of areas with different depths. Three case studies were employed to demonstrate the method's ability and effectiveness in accurately detecting features. Results show that a feature recognition success rate of 100% was achieved for the case studies, implying that the developed method for blind pocket and island detection is effective and reliable.

Keywords: *CNC; milling machine; geometric information; STEP AP242; feature recognition; blind pocket; island*

1. Introduction

Feature recognition is a fundamental process in identifying attributes in Standard for the Exchange of Product Model Data (STEP) files. These files are widely used for generating the G-code for computer numerical control (CNC) machining because they provide standardised platforms for data exchange between computer-aided design (CAD), computer-aided manufacturing (CAM) and CNC systems. The files eventually help minimise data loss during transmission [1], [2]. A CNC machine is used to machine workpieces made of various materials, including metals and nonmetals, through the movements of the CNC apparatus [3]–[5]. Previous scholars have investigated the utilisation of a STEP file as a primary data source. Their emphasis lies in applying the STEP file to their enquiry related to straight lines, curves and profiles. A straight line represents the movement of toolpaths in a linear fashion. By contrast, a curve signifies the movement of toolpaths in a curvilinear manner, either to the right or to the left. The profile indicates the integration of the line and curve [6]–[9]. All these investigations focused on the Cartesian coordinate system, which facilitates the generation of lines, curves and profiles. In another study, researchers employed a STEP AP242 file, concentrating on rectangular blind pockets [10]. The STEP file served as the input, blind pockets and islands were identified through a geometric identification method and multidepth analysis was utilised for blind pocket and island evaluation.

STEP AP242 represents a significant advancement over other STEP application protocols. AP203 and AP214 are the closest examples. AP203 supports basic geometries and configuration data, whilst AP214 extends the capabilities to include automotive-specific design information. Both protocols, however, are limited in their ability to provide comprehensive semantic representation of manufacturing intent [11]. STEP AP242 integrates geometry, topology [12] and product manufacturing information (PMI) into a unified and semantically enriched data structure [13]. This integration enables a more reliable interpretation of feature boundaries, depth relationships and surface hierarchies, which are essential for automated feature recognition. Consequently, STEP AP242 is particularly well suited for feature-based reasoning and serves as a robust input format for the proposed blind pocket and island recognition methodology.

1.1 Structure of STEP File

Another name for STEP is ISO 10303, which is the standard for design and manufacturing applications [14]. STEP files were introduced to standardise the exchange of technical specification data in machining applications [15]. They also facilitate lossless data transfer between different CAD systems, such as Autodesk Inventor, SolidWorks and other compatible software platforms [16]. All these software platforms can be used to produce and read the shared STEP file and reproduce it in each software. The ability to accurately share and utilise STEP files enhances the overall efficiency of the design and manufacturing processes, enabling optimal collaboration amongst engineers and designers [17]. On the contrary, the lack of a standardised STEP file can contribute to increased machining time, machining errors and costs [18]. The generated G-code is executed by the CNC machine to control the tool movement along the predefined toolpath [19], [20].

The STEP file data structure in Figure 1 for a CNC milling machine contains a CLOSED_SHELL entity. It represents the closed surfaces formed by a set of interconnected boundaries arranged by Cartesian points [21]. CLOSED_SHELL is essential for describing the solid geometry of a workpiece in a STEP file through a series of Cartesian points [22], [23]. These Cartesian points provide the geometric data required for defining the dimensions, boundaries and topology of the workpiece. Blind pockets and islands can be identified and extracted by analysing these geometric data manufacturing features. Therefore, STEP files formed the basis of the feature recognition process investigated in this study. Three case studies involving workpieces with different features were adopted.

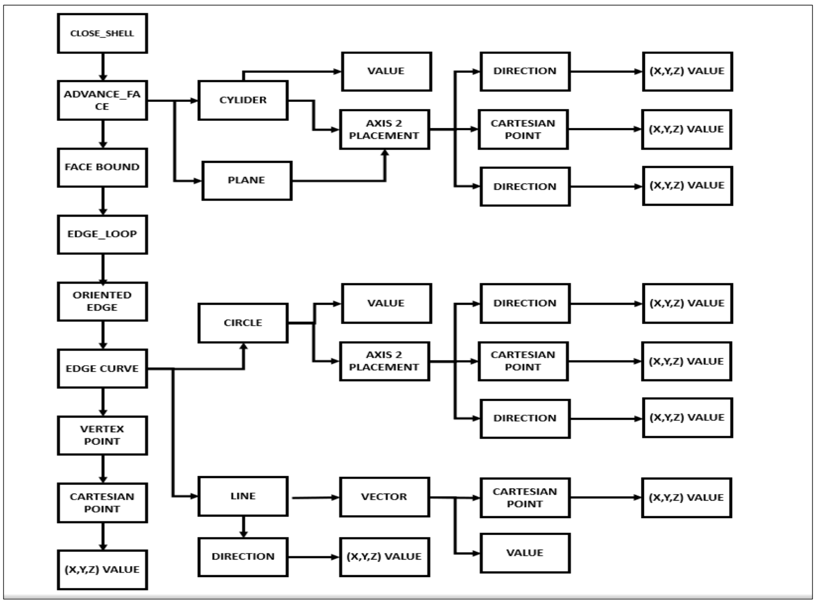

Fig. 1. STEP file data structure

2. Methodology

2.1. Data Acquisition

The STEP AP242 files used in this study were obtained from SolidWorks CAD software. After the design was finalised, the files were saved in STEP AP242 format, which contained the geometric data necessary for identifying blind pockets and islands. Three case studies were developed in this research: Case Study 1, Case Study 2 and Case Study 3. All case studies used the same workpiece dimension with a length and width of 100 mm and a thickness of 24 mm. Each case study consisted of one island and one blind pocket in a single workpiece.

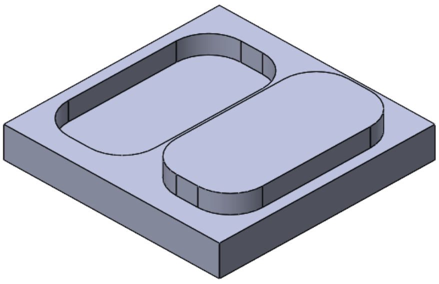

Fig. 2. Case Study 1: same size, centred location, island pocket

Figure 2 shows the first case study. The workpiece was designed with an island and a blind pocket. The island and pocket measured 80 mm in length and 40 mm in width. Both had a height of 9 mm, with each corner featuring a radius of 15 mm. The centre of the island was located 75 mm along the Y-axis and 50 mm along the X-axis. The centre of the pocket was positioned 25 mm in the Y-axis and 50 mm in the X-axis.

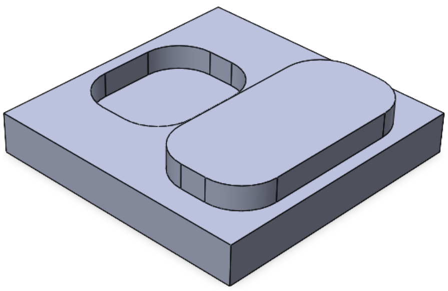

Fig. 3. Case Study 2: different sizes, centred location, island pocket

Figure 3 illustrates the second case study. The overall workpiece dimensions remained unchanged. However, variations were introduced in the size and position of the features. The island features had the same dimensions as in the first case study: 80 mm in length, 40 mm in width and 9 mm in height, with a corner radius of 15 mm. However, in this case, the centre of the island was positioned 25 mm from the Y-axis and 50 mm from the X-axis of the workpiece. The blind pocket in this case was smaller than that in the first case, measuring 50 mm in length, 40 mm in width, 9 mm in depth and 15 mm in corner radius. The centre of the blind pocket was located 75 mm from the Y-axis and 50 mm from the X-axis of the workpiece. This positioning was crucial for evaluating how the recognition method handles features of different sizes in the workpiece.

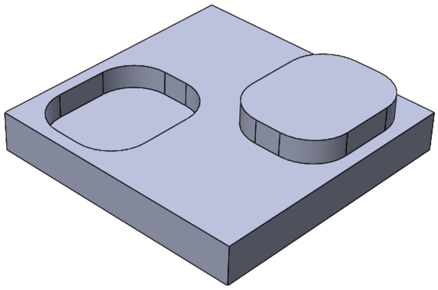

Fig. 4. Case Study 3: same size, different locations, island pocket

Figure 4 shows the third case study. This study explored the capabilities of the recognition method by incorporating smaller island and blind pocket. The island feature had dimensions of 50 mm in length, 40 mm in width and 9 mm in height, with a corner radius of 15 mm. The centre of the island was located at 75 mm on the X-axis and 25 mm on the Y-axis. The blind pocket had the following measurements: a length of 50 mm, a width of 40 mm, a depth of 9 mm and a corner radius of 5 mm. The centre of the blind pocket was positioned at 25 mm on the X-axis and 75 mm on the Y-axis. This configuration presented a challenging case for feature recognition given the relatively small feature size and closeness to the workpiece edge.

2.2. Feature Recognition Method

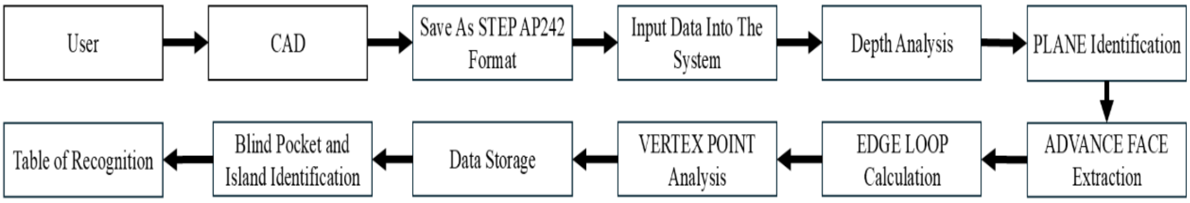

Fig. 5. Feature recognition method

Figure 5 shows the steps for recognising blind pocket and island features used in this research. Firstly, a 3D CAD model was built in SolidWorks and saved as STEP AP242. When this step was complete, STEP file generation began. The process of producing a STEP file is depicted in Figure 6.

Fig. 6. STEP file production

The STEP file data were then entered into the system and stored in the database. The next step was depth analysis, followed by the identification of the PLANE. Subsequently, the ADVANCE_FACE extraction process was performed and the EDGE_LOOP was calculated. The VERTEX_POINT analysis was conducted afterwards. Once all data were collected, they were stored for further processing. Finally, the blind pocket and island were recognised, leading to the creation of the 'Table of recognition' in Table 1.

2.3. Depth Analysis

Firstly, the Z-axis value from the Cartesian point of the STEP file was determined to find the object depth. Next, the minimum and maximum Z-axis values, which were -24 and 0, respectively, from the STEP file were excluded. Meanwhile, the remaining Z-axis values, which were −9 and −18, were taken into consideration to determine the depth of the objects. Then, the values were input into the array database, where they could be retrieved. Finally, the unique values for the blind pocket and island features were extracted. The blind pocket and island were determined using the table of recognition.

2.4. Advanced Face Extraction

The ADVANCED_FACE was determined using the values obtained from the PLANE. Figure 7 illustrates the flowchart for obtaining the ADVANCE_FACE value.

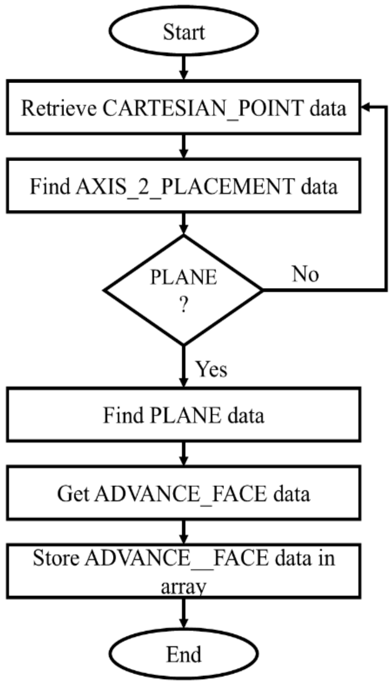

Fig. 7. ADVANCE_FACE extraction flowchart

Case Study 1 indicated that the #value for plane #651 was defined as PLANE ('', #650). The advanced face was found using #651, resulting in

#688 = ADVANCED_FACE (", (#671, #677, #687), #651, .T.). The values in the brackets represented the face bounds and were stored accordingly.

Next, Case Study 2 showed that the #value for plane #343 was PLANE (", #342). The advanced face was identified using #343, resulting in #472 = ADVANCED_FACE (", (#403, #428, #471), #343, .T.). Then, the values in the brackets were stored.

Finally, in Case Study 3, the #value for plane #467 was PLANE (", #466). The advanced face was found using #466, leading to #564 = ADVANCED_FACE (", (#509, #520, #563), #467, .T.). The values in the brackets were also stored.

2.5. Edge Loop Calculation

The edge loop calculation determined the number of data points within edge loops, selecting the loop with the highest count for further analysis. The flowchart is shown in Figure 8.

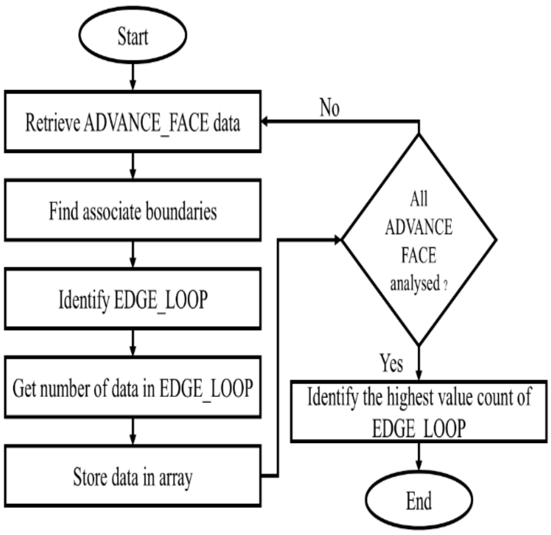

Fig. 8. Edge loop calculation flowchart

In Case Study 1, the advanced face was represented as #688 = ADVANCED_FACE (", (#671, #677, #687), #651, T.), indicating three values: #671, #677 and #687. The analysis began with #671, whose face boundary was #671 = FACE_BOUND (", #670, .T.), linking it to boundary #670. With #670, the edge loop was identified as #670 = EDGE_LOOP (", (#652, #653, #654, #660, #661, #662, #663, #669)).

In Case Study 2, the advanced face was represented as #472 = ADVANCED_FACE(", (#403, #428, #471), #343, .T.), containing values #403, #428 and #471. The analysis started with #403, whose face boundary was #403 = FACE_BOUND (", #402, .T.), linking it to boundary #402. The corresponding edge loop was identified as #402 = EDGE_LOOP (", (#344, #352, #361, #369, #378, #386, #395, #401).

In Case Study 3, the advanced face was represented as #564 = ADVANCED_FACE (", (#509, #520, #563), #467, .T.), containing values #509, #520 and #563. The analysis began with #563, whose face boundary was #563 = FACE_BOUND (", #562, .T.), linking it to boundary #562. The edge loop was identified as #562 = EDGE_LOOP (", (#528, #535, #536, #537, #545, #554, #560, #561)). All data contained within the edge loop bracket will undergo further analysis.

2.6. Vertex Point Analysis

The edge curves consisted of three data points: two representing vertex points and one defining either a circle or a line. The vertex point values were used to retrieve the corresponding Cartesian point values. If the edge curve represented a circle, AXIS2_PLACEMENT_3D was utilised to determine the Cartesian points. For lines, the first value corresponded to the Cartesian point, whilst the second value indicated the vector direction.

Firstly, vertex point analysis was performed, in which VERTEX_POINTS were recognised and analysed to know the importance of their roles in the geometric structure. Secondly, ORIENTED_EDGES were located, followed by finding the EDGE_CURVES generated by the edges. Whether any EDGE_CURVES represent a CIRCLE or LINE was determined. If an edge was identified as a circle, its radius was analysed together with the associated AXIS2_PLACEMENT_3D to determine the 3D orientation of the geometry. Otherwise, the edge was classified as a line. The Cartesian points were then located and stored in an array. The process concluded with a clear set of data points for the next phase of analysis stages.

For Case Study 1, the analysis began with edge loop #670, defined as #670 = EDGE_LOOP (", (#652, #653, #654, #660, #661, #662, #663, #669)). This loop included multiple oriented edges: #652, #653, #654, #660, #661, #662, #663 and #669. Oriented edge #652 was linked to edge curve #318, connecting vertices #310, #312 and #317. Vertex #310 corresponded to Cartesian point #309 at (90., 30., −9 .) and #312 corresponded to #311 at (75., 45., −9 .). Edge curve #317 represented a circle with a radius of 15, defined by #316, an AXIS2_PLACEMENT_3D at Cartesian point #313 (75., 30., −9 .). The orientation of this circle was defined by the axis placement, outlining a curved section within the edge loop.

Next, oriented edge #653 was associated with edge curve #451, connecting vertices #354, #310 and #450. Vertex #354 corresponded to Cartesian point #353 at (90., 20., −9 .), whilst #310 corresponded to #309 (90., 30., −9 .). Edge curve #450 was a straight line defined by points #447 and #449, with #447 located at (90, 20, −9).

For Case Study 2, the analysis started with edge loop #402, defined as #402 = EDGE_LOOP('', (#344, #352, #361, #369, #378, #386, #395, #401)). This loop consisted of multiple oriented edges: #344, #352, #361, #369, #378, #386, #395 and #401. Oriented edge #344 was associated with edge curve #41, connecting vertices #33, #35 and #40. Vertex #33 corresponded to Cartesian point #32 at (75., 30., −9 .) and #35 corresponded to point #34 at (60., 45., −9 .). Edge curve #40 was a circle with a radius of 15, defined by #39, which represented an AXIS2_PLACEMENT_3D at #36, located at (60., 30., −9 .). Next, oriented edge #352 was associated with edge curve #351, connecting vertices #346, #33 and #350. Vertex #346 corresponded to Cartesian point #345 at (75., 20., −9 .), whilst #33 corresponded to #32 at (75., 30., −9 .). Edge curve #350 was a straight line defined by points #347 and #349, with #347 located at (75., 20., −9 .).

Finally, in Case Study 3, the analysis began with edge loop #562. This edge loop consisted of several oriented edges: #528, #535, #536, #537, #545, #554, #560 and #561. In particular, oriented edge #528 was linked to edge curve #527, which connected vertices #522, #438 and #526. Vertex #522 corresponded to Cartesian point #521 at (55., 70., −9 .) and vertex #438 corresponded to #437, located at (55., 80., −9 .). Edge curve #526 was a line defined by points #523 and #525, with #523 located at (55., 70., −9 .). Next, oriented edge #535 was associated with edge curve #534, which connected vertices #321, #522 and #533. Vertex #321 corresponded to Cartesian point #320 at (40., 55., −9 .), whilst vertex #522 corresponded to #521 at (55., 70., −9 .). Edge curve #533 represented a circle, with #532 being AXIS2_PLACEMENT_3D defined by points #529, #530 and #531. Cartesian point #529 was located at an X-axis value of 40, a Y-axis value of 70 and a Z-axis value of −9 , setting the orientation of the circle within the 3D space.

This analysis captured linear and circular parameters from the STEP file, using Cartesian points and axis placements to determine the geometric structure and ensure a comprehensive understanding of the edge loop's configuration and its relationships. The process was repeated until all #values were analysed.

2.7. Data Storage

Data storage refers to storing data collected using other processes for future purposes. In this case, the raw data collected from the STEP file were saved in tables in the MySQL database. The required data were retrieved from the database for use in the process. The extracted geometric data and processing results were organised into arrays to facilitate efficient access during subsequent analysis. Cartesian coordinates were stored within these data structures for feature identification and evaluation. This procedure was performed for all other data related to the advanced face. Various arrays were utilised to ensure proper data storage.

2.8. Blind Pocket and Island Identification

An identification process was conducted to determine the type of feature in each model, whether a blind pocket or an island, to validate the case studies. The flowchart for the identification process is shown in Figure 9.

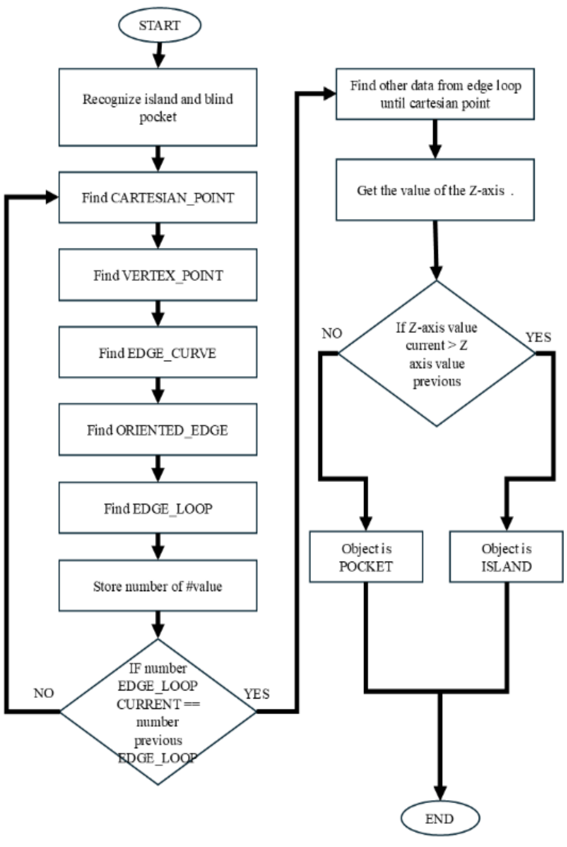

Fig. 9. Blind pocket and island identification flowchart

Following the data collection process, a Cartesian point was selected from the database on the basis of its X and Y coordinate values. The system then scanned the database and retrieved the related vertex point, edge curve, oriented edge and edge loop information. The number of entities within the edge loop was subsequently determined. If the identified edge loop data matched to the previously selected edge loop, that edge loop was retained for further analysis. Afterwards, the Z-axis value of the selected edge loop was evaluated and compared with the reference value. If it was higher than the previous value, it represented an island feature; by contrast, a lower Z-axis value showed a blind pocket feature.

3. Results

Table 1 presents the recognition result used to validate the method for identifying blind pocket and island features in a STEP file on the basis of Z-axis value comparisons. The results were structured in accordance with the case studies, with each case study containing several groups distinguished by the respective Z-coordinates. For example, Case Study 1 contained Group 1 ($Z = -9$), Group 2 ($Z = -9$), Group 3 ($Z = 0$) and Group 4 ($Z = -18$). In this regard, classifications included labels such as ‘Plane (blind Pocket)’, ‘Plane (Island)’, ‘Island’ or ‘blind Pocket’. This result provided opportunities to evaluate how this approach recognises zones within 3D CAD models.

The results indicated that a Z-axis value of −9 acted as the reference plane between blind pocket and island features. Regions with Z-axis greater than −9 , such as Z = 0, were identified as islands, whereas regions with Z-axis lower than −9 , such as Z = −18, were identified as blind pockets.

A consistent classification pattern was observed in all three case studies, indicating the reliability of this approach in geometric feature recognition in CAD models. No inconsistencies were found in the labels across coordinate values. In each of the tests, the island and blind pocket were identified accurately. These findings further support the effectiveness of the recognition depicted in Figure 9 for distinguishing between blind pocket and island features within STEP-based CAD models.

Table 1,
Table of recognition

Case study	Result	Group 1: Z = −9	Group 2: Z = −9	Group 3: Z = 0	Group 4: Z = −18
1		#309: (90., 30., −9.)	#286: (90., 70., −9.)	#236: (75., 95., 0.)	#320: (75., 45., −18.)
		#353: (90., 20., −9.)	#174: (75., 55., −9.)	#238: (25., 95., 0.)	#567: (25., 45., −18.)
		#351: (75., 5., −9.)	#166: (25., 55., −9.)	#196: (10., 80., 0.)	#559: (10., 30., −18.)
		#395: (25., 5., −9.)	#214: (10., 70., −9.)	#198: (10., 70., 0.)	#412: (10., 20., −18.)
		#393: (10., 20., −9.)	#206: (10., 80., −9.)	#156: (25., 55., 0.)	#404: (25., 5., −18.)
		#550: (10., 30., −9.)	#254: (25., 95., −9.)	#154: (75., 55., 0.)	#370: (75., 5., −18.)
		#548: (25., 45., −9.)	#246: (75., 95., −9.)	#276: (90., 70., 0.)	#362: (90., 20., −18.)
		#311: (75., 45., −9.)	#502: (90., 80., −9.)	#493: (90., 80., 0.)	#328: (90., 30., −18.)
	Result	Plane (Pocket)	Plane (Island)	Island	Pocket
2		#32: (75., 30., −9.)	#124: (90., 70., −9.)	#295: (75., 95., 0.)	#43: (60., 45., −18.)
		#345: (75., 20., −9.)	#163: (75., 55., −9.)	#304: (25., 95., 0.)	#230: (40., 45., −18.)
		#353: (60., 5., −9.)	#206: (25., 55., −9.)	#312: (10., 80., 0.)	#238: (25., 30., −18.)
		#362: (40., 5., −9.)	#198: (10., 70., −9.)	#187: (10., 70., 0.)	#247: (25., 20., −18.)
		#370: (25., 20., −9.)	#438: (10., 80., −9.)	#189: (25., 55., 0.)	#255: (40., 5., −18.)
		#379: (25., 30., −9.)	#446: (25., 95., −9.)	#154: (75., 55., 0.)	#264: (60., 5., −18.)
		#387: (40., 45., −9.)	#455: (75., 95., −9.)	#114: (90., 70., 0.)	#272: (75., 20., −18.)
		#34: (60., 45., −9.)	#132: (90., 80., −9.)	#116: (90., 80., 0.)	#51: (75., 30., −18.)
	Result	Plane (Pocket)	Plane (Island)	Island	Pocket
3		#521: (55., 70., −9.)	#468: (95., 30., −9.)	#76: (40., 95., 0.)	#253: (80., 45., −18.)
		#320: (40., 55., −9.)	#344: (95., 20., −9.)	#85: (20., 95., 0.)	#262: (60., 45., −18.)
		#51: (20., 55., −9.)	#342: (80., 5., −9.)	#93: (5., 80., 0.)	#158: (45., 30., −18.)
		#43: (5., 70., −9.)	#484: (60., 5., −9.)	#32: (5., 70., 0.)	#150: (45., 20., −18.)
		#538: (5., 80., −9.)	#142: (45., 20., −9.)	#34: (20., 55., 0.)	#278: (60., 5., −18.)
		#546: (20., 95., −9.)	#140: (45., 30., −9.)	#109: (40., 55., 0.)	#287: (80., 5., −18.)
		#445: (40., 95., −9.)	#407: (60., 45., −9.)	#117: (55., 70., 0.)	#295: (95., 20., −18.)
		#437: (55., 80., −9.)	#405: (80., 45., −9.)	#74: (55., 80., 0.)	#251: (95., 30., −18.)
	Result	Plane (Pocket)	Plane (Island)	Island	Pocket

As shown in Table 2, no variation was observed in the samples of ADVANCE_FACE or reference #739 for CLOSED_SHELL i across all case studies presented.

Although all three case studies shared the same value for ADVANCE_FACE (24), the values for CLOSED_SHELL differed because each case study represented a unique geometric configuration. The differences occurred because of the variations in feature size and location within the workpiece.

Table 2,
Case study comparisons

Case study	Reference number	Total ADVANCE_FACE	CLOSED_SHELL
1	#739	24	#66,#97,#128,#150,#190,#230,#270,#303,#345,#387,#429,#441,#463,#487,#518,#542,#584,#606,#624,#646,#688,#705,#722,#738
2	#739	24	#68,#108,#148,#181,#223,#289,#338,#472,#496,#520,#542,#564,#586,#603,#620,#637,#649,#661,#673,#685,#697,#714,#726,#738
3	#739	24	#68,#134,#174,#214,#245,#312,#336,#368,#399,#430,#462,#564,#581,#598,#615,#627,#644,#656,#673,#690,#702,#714,#726,#738

4. Discussion

The results obtained from the case studies show that the proposed depth-based recognition method is capable of successfully identifying blind pocket and island features. The use of Z-axis depth analysis, together with geometric and topological entities extracted from STEP AP242 files, enables accurate feature classification. The consistent feature recognition demonstrates the robustness of the methodology for prismatic parts with non-overlapping features, compared with a conventional feature recognition approach, which relies on complex graph-based reasoning. The proposed method provides a simpler, computationally efficient solution by using depth relationships and edge loop structure. However, this study is limited to the recognition of prismatic features. As such, the proposed approach does not intend to analyse complex, curved surfaces or free-form shapes found in advanced industrial components. The primary purpose of this study was to validate the fundamental feature recognition mechanism based on depth layer extraction and EDGE_LOOP interpretation. The handling of intersecting features, multidepth hierarchies and nonprismatic geometries will be addressed in future extensions of the methodology.

5. Conclusions

On the basis of the analysis presented, the proposed methodology for detecting blind pocket and island features was found to be effective. This finding is validated by the successful identification of these features across all three cases presented. The case studies demonstrated that the algorithm can accurately recognise and classify geometric regions on the basis of their depth characteristics. Furthermore, the method consistently differentiated between blind pockets and islands under varying Z-coordinate values, confirming the reliability of the proposed approach for feature recognition in STEP-based CAD models. Despite its strengths, this methodology has several limitations: Geometric features must not overlap and slanted and curved surfaces cannot be processed using this methodology. The future work will upgrade the methodology to handle more complex geometries, variable-depth interactions and broader industrial use cases.

Conflict of Interest

The authors declare that there is no conflict of interest regarding the publication of this paper.

Acknowledgement

The author gratefully acknowledges the support, facilities and research environment provided by Universiti Sultan Zainal Abidin (UniSZA) throughout this research. The author also thanks all individuals who contributed to the successful completion of the research.

Funding

This work wass funded by the UniSZA industry grant UniSZA/2023/PPL/WENTEC (031).

References

[1] Monir, Koura., Omar, Koura., Tamer, Sayed. Geometric data extraction methodology from step file for cylindrical parts. Journal of Al-Azhar University Engineering Sector, no. 71 698–708, 2024. https://doi.org/10.21608/auej.2024.259608.1580.

[2] Uddin, Mohammad Moin, Keith Johnson, and Craig Leendert. CAD OER - Equity in Access for Engineering/Engineering Tech Students Paper presented at 2023 CIEC, Charleston, South Carolina. https://doi.org/10.18260/1-2-1153-48792

[3] Mohsen, Soori., Behrooz, Arezoo., Roza, Dastres. (2024). Sustainable CNC Machining Operations, A Review. Sustainable operations and computers, volume 5 2024. https://doi.org/10.1016/j.susoc.2024.01.001

[4] Mohsen, Soori., Fooad, Karimi, Ghaleh, Jough., Roza, Dastres., Behrooz, Arezoo. Robotical Automation in CNC Machine Tools: A Review. Acta Mechanica et Automatica, 18(3), 434-450,2024. https://doi.org/10.2478/ama-2024-0048

[5] Latif, Kamran, Yusri Yusof, and Aini Zuhra Abdul Kadir. "Development of new integrated CNC system for ISO6983 data interface model."International Journal on Interactive Design and Manufacturing (IJIDeM): 1-9, 2022. https://doi.org/10.1007/s12008-021-00837-2

[6] Ibrahim, Z., S. B. Mohamed, M. Minhat, A. S. Mohamed, M. R. Musanih, Z. Abd Rahman, and Zairi Ismael Rizman. "Reason maintenance in product modelling via open source CAD system." International Journal on Advanced Science, Engineering and Information Technology, no. 6, 990-996, 2016. https://doi.org/10.18517/ijaseit.6.6.953

[7] Sharizam, Muhammad Abdulrahim Rabbani Md, Saiful Bahri Mohamed, Tengku Mohd Shahrir Tengku Sulaiman, Zammeri Abd Rahman, and Roslan Awang. "Development of the PC-based Integrated Interface System of STEP file for CNC Machining Application: Circular Features."International Journal of Integrated Engineering12, no. 7 195-203,2020. https://doi.org/10.30880/ijie.2020.12.07.022

[8] Abd Rahman, Z., S. B. Mohamed, M. S. Kasim, M. K. A. Arifffn, and A. R. Zulkifli. "The Development of Methodology for Tool Path Generation Using STEP Data Model Based on ISO 6983."International Journal of Engineering Trends and Technology69, no. 6, 144-153, 2021. https://doi.org/10.14445/22315381/IJETT-V69I6P222

[9] Sulaiman, TMS Tg, S. B. Mohamed, M. Minhat, A. S. Mohamed, and A. R. Mohamed. "Integrated Interface Development Environment using STEP Universal Data Structure." International Journal of Engineering & Technology 7, no. 2.15, 27-29, 2018. https://doi.org/10.14419/ijet.v7i2.15.11194

[10] Abd Rahman, Zammeri, Saiful Bahri Mohamed, Mohammad Minhat, Alias Mohd, and Zulkifli Abd Rahman. "Integrated Interface System of STEP Data Models for the Tool Path Generation." International Journal of Integrated Engineering 14, no. 4, 160-170, 2022. https://doi.org/10.30880/ijie.2022.14.04.012

[11] S. K. Mohammed, M. H. Arbo, and L. Tingelstad, "Leveraging model based definition and STEP AP242 in task specification for robotic assembly," 2020. https://doi.org/10.1016/j.procir.2020.05.209

[12] B. Song, J. Pierre, D. Peters, and K. Tobias, "Heliyon Geometric feature extraction in manufacturing based on a knowledge graph," *HLY*, vol. 9, no. 9, 2023. https://doi.org/10.1016/j.heliyon.2023.e19694

[13] Chen, Y, H Wang, L Wang, S Xu, L Liao, J Mo, and X Lin., "Three-Dimensional Visualization of Product Manufacturing Information in a Web Browser Based on STEP AP242 and WebGL," *Appl. Sci.*, vol. 15, no. 19, 2025. https://doi.org/10.3390/app151910847

[14] Sarkar, Arkopaul, and Dušan Šormaz. "On semantic interoperability of model-based definition of product design." Procedia Manufacturing 38 513-523, 2019. https://doi.org/10.1016/j.promfg.2020.01.065

[15] Zammeri, Abd Rahman, Saiful, Bahri, Mohamed, Mohamad, Minhat, Alias, Mohd, Zulkifli, Abd Rahman, Roslan, Awang. G-code converter using interface system for a STEP file (ISO 10303). Indonesian Journal of Electrical Engineering and Computer Science, 31(3), 1362-1362, 2023. http://doi.org/10.11591/ijeecs.v31.i3.pp1362-1371

[16] Zhu, Wendan, Tianliang Hu, Weichao Luo, Yan Yang, and Chengrui Zhang. "A STEP-based machining data model for autonomous

process generation of intelligent CNC controller." The International Journal of Advanced Manufacturing Technology 96, 271-285, 2018. https://doi.org/10.1007/s00170-017-1554-9

[17] Bitla, Venu., Venkateswara, Rao, Komma. STEP-based feature recognition from solid models having non-planar surfaces. International Journal of Computer Integrated Manufacturing, 30(10), 1011-1028, 2017. https://doi.org/10.1080/0951192X.2016.1268719

[18] Fusaomi, Nagata., Yusaku, Yamane., Yudai, Okada., Takamasa, Kusano., Keigo, Watanabe., Maki, K., Habib. Development of a post-processor approach for an industrial robot, FANUC R2000iC. Artificial Life and Robotics, 23(2), 186-191, 2018. https://doi.org/10.1007/S10015-017-0411-0

[19] Qinbo, Li., Sheng-Jen, Hsieh. An intelligent tutoring system for computer numerical control programming. International Journal of Engineering Education, 35(1), 252-261. 2019. https://api.semanticscholar.org/CorpusID:145933075

[20] Kamran, Latif., Anbia, Adam., Yusri, Yusof., Aini, Zuhra, Abdul, Kadir. A review of G code, STEP, STEP-NC, and open architecture control technologies based embedded CNC systems. The International Journal of Advanced Manufacturing Technology, 114(9), 2549-2566, 2021. https://doi.org/10.1007/s00170-021-06741-z

[21] Sreeramulu Dowluru, Suman P, and Satish Kumar Adapa. "A New Methodology to Extract Machining Features from Prismatic Parts." International Conference on Advances in Engineering and Technology (ICAET'2014), 29-30, 2014. http://dx.doi.org/10.15242/IIE.E0314081

[22] Abd Rahman, Z., Mohamed, S. B., Minhat, M., & Abd Rahman, Z. Design and development of 3-axis Benchtop CNC milling machine for educational purpose. International Journal of Integrated Engineering, 15(1), 145-160, 2023. https://doi.org/10.30880/ijie.2023.15.01.013

[23] Omar, Muhammad Haziq, Siti Nurul Akmal Yusof, Saiful Bahri Mohamed, Amirulihsan Mohamad, Raja Fatin Najiha Raja Anuar, Zammeri Abd Rahman, Yutaka Asako, and Huang Da. "Milling Features Recognition Methodology of Rectangular Fillet Blind Pocket for Universal Data Structure." Journal of Advanced Research in Applied Sciences and Engineering Technology 30, no. 3 57-68, 2023. https://doi.org/10.37934/araset.30.3.5768.

التعرف على السمات القائمة على العمق للجيوب والجزر المخفية من نماذج CAD وفقًا لمعيار STEP AP242 لتطبيقات الطحن

Amirulihsan Mohamad[1], Zammeri Abd Rahman[2*], Saiful Bahri Mohamed Mohamad[3], Muhammad Haziq Omar[4], Razwan Rohimi[5], Muhammad Abdulrahim Rabbani Md Sharizam[6], Tengku Mohd Sharir Tengku Sulaiman[7], Mohamad Minhat[8] and Wawan Trisnadi Putra[9]

[1,2,3,4,5,6,7]*Design Optimization and Manufacturing Research Group, Faculty of Innovative Design and Technology, Universiti Sultan Zainal Abidin, Kampus Gong Badak, 21300 Kuala Nerus, Terengganu, Malaysia*
[8]*Faculty of Manufacturing Engineering, Universiti Teknikal Malaysia Melaka, Hang Tuah Jaya, 76100 Durian Tunggal, Melaka, Malaysia*
[9]*Faculty of Engineering, Universitas Muhammadiyah Ponorogo, Ponorogo 63471, Indonesia*
*Corresponding Author's E-mail: zammeri@unisza.edu.my

المستخلص

يُعد تحديد ملامح الجيوب العمياء والجزر في التصميم الحديث بمساعدة الحاسوب (**CAD**) وفي تصنيع نماذج **CAD** ثلاثية الأبعاد أمرًا بالغ الأهمية. فهو يضمن الدقة والكفاءة في عملية التصنيع باستخدام التحكم الرقمي بالحاسوب (**CNC**). وغالبًا ما تشكل هذه الملامح تحديات أمام عملية الكشف الآلي. تقترح هذه الدراسة طريقة آلية للكشف عن الجيوب العمياء والجزر في ملفات **AP242** الخاصة بمعيار تبادل بيانات نماذج المنتجات (**STEP**) باستخدام نهج قائم على العمق. تتضمن المنهجية تحليل المعلومات الهندسية من ملف **STEP**، وترتيب المناطق حسب العمق (قيم **Z**)، والتمييز بين ميزات الجيوب العمياء والجزر. يستخدم هذا النهج سلسلة من الخوارزميات الهندسية للكشف عن الحواف والرؤوس والأسطح، يليها تحديد المناطق ذات الأعماق المختلفة. وقد تم استخدام ثلاث دراسات حالة لإثبات قدرة هذه الطريقة وفعاليتها في الكشف الدقيق عن السمات. وتُظهر النتائج أنه تم تحقيق معدل نجاح في التعرف على السمات بنسبة ١٠٠٪ في دراسات الحالة، مما يشير إلى أن الطريقة المطورة للكشف عن الجيوب العمياء والجزر فعالة وموثوقة.